Neurobiology of Disease

Short Amyloid-β (Aβ) Immunogens Reduce Cerebral Aβ Load and Learning Deficits in an Alzheimer's Disease Mouse Model in the Absence of an Aβ-Specific Cellular Immune Response

Marcel Maier,[1] Timothy J. Seabrook,[1] Noel D. Lazo,[2] Liying Jiang,[1] Pritam Das,[3] Christopher Janus,[3] and Cynthia A. Lemere[1]

[1]Center for Neurological Diseases, Brigham and Women's Hospital, Harvard Medical School, Boston, Massachusetts 02115, [2]Department of Neurology, David Geffen School of Medicine at the University of California, Los Angeles, Los Angeles, California 90095, and [3]Department of Neuroscience, Mayo Clinic Jacksonville, Jacksonville, Florida 32224

Amyloid-β (Aβ) immunotherapy lowers cerebral Aβ and improves cognition in mouse models of Alzheimer's disease (AD). A clinical trial using active immunization with Aβ1–42 was suspended after ~6% of patients developed meningoencephalitis, possibly because of a T-cell reaction against Aβ. Nevertheless, beneficial effects were reported in antibody responders. Consequently, alternatives are required for a safer vaccine. The Aβ1–15 sequence contains the antibody epitope(s) but lacks the T-cell reactive sites of full-length Aβ1–42. Therefore, we tested four alternative peptide immunogens encompassing either a tandem repeat of two lysine-linked Aβ1–15 sequences (2×Aβ1–15) or the Aβ1–15 sequence synthesized to a cross-species active T1 T-helper-cell epitope (T1-Aβ1–15) and each with the addition of a three-amino-acid RGD (Arg-Gly-Asp) motif (R-2×Aβ1–15; T1-R-Aβ1–15). High anti-Aβ antibody titers were observed in wild-type mice after intranasal immunization with R-2×Aβ1–15 or 2×Aβ1–15 plus mutant *Escherichia coli* heat-labile enterotoxin LT(R192G) adjuvant. Moderate antibody levels were induced after immunization with T1-R-Aβ1–15 or T1-Aβ1–15 plus LT(R192G). Restimulation of splenocytes with the corresponding immunogens resulted in moderate proliferative responses, whereas proliferation was absent after restimulation with full-length Aβ or Aβ1–15. Immunization of human amyloid precursor protein, familial AD ($hAPP_{FAD}$) mice with R-2×Aβ1–15 or 2×Aβ1–15 resulted in high anti-Aβ titers of noninflammatory T-helper 2 isotypes (IgG1 and IgG2b), a lack of splenocyte proliferation against full-length Aβ, significantly reduced Aβ plaque load, and lower cerebral Aβ levels. In addition, 2×Aβ1–15-immunized $hAPP_{FAD}$ animals showed improved acquisition of memory compared with vehicle controls in a reference-memory Morris water-maze behavior test that approximately correlated with anti-Aβ titers. Thus, our novel immunogens show promise for future AD vaccines.

Key words: **Alzheimer's disease; amyloid beta; Aβ peptide; immunotherapy; behavior; T-cell; intranasal**

Introduction

Alzheimer's disease (AD) is characterized histopathologically by accumulation of amyloid plaques and neurofibrillary tangles with amyloid-β peptide (Aβ) as a major component of AD-related plaques. Numerous evidence indicate that different forms of Aβ aggregates play an important role in AD pathogenesis (Hardy and Selkoe, 2002; Walsh and Selkoe, 2004). This led to experimental therapeutic strategies for AD to reduce cerebral Aβ by generating antibodies against Aβ1–42 (Schenk et al., 1999). In AD mouse models, immunization with aggregated synthetic Aβ1–42 peptide reduced cerebral Aβ deposition, neuritic dystrophy, and gliosis in amyloid precursor protein-transgenic (APP-tg) mice (Schenk et al., 1999; Lemere et al., 2000; Weiner et al., 2000) and also improved cognition (Janus et al., 2000; Morgan et al., 2000). A clinical study in AD patients using aggregated Aβ1–42 (AN1792) in combination with QS21 adjuvant was halted because of signs of meningoencephalitis in ~6% of immunized subjects (Orgogozo et al., 2003). Nevertheless, patients who generated anti-Aβ antibodies had reduced cerebrospinal levels of tau and showed a slower cognitive decline (Gilman et al., 2005; Masliah et al., 2005). T-cell infiltrates were present in the brains of two patients with encephalitis, suggesting a T-cell-mediated immune response as a reason for the adverse events (Nicoll et al., 2003; Ferrer et al., 2004).

Received Jan. 26, 2006; revised March 9, 2006; accepted March 20, 2006.

This work was supported by National Institutes of Health Grant AG20159 (C.A.L.). We thank Diana Li, Elaina Mikhaylova, Eva Luo, and Katelyn Thomas for technical assistance, Todd Golde for the determination/confirmation of Aβ levels in brain homogenates, Lucy Cardenas-Freytag and John D. Clements for adjuvant LT(R192G), Dennis Selkoe for the gift of R1282 antibodies, Jie Shen for the use of the behavioral testing Morris water maze facility, Guiquan Chen for assistance with the statistical data analysis, and Lennart Mucke for sharing the $hAPP_{FAD}$ (J20) transgenic mouse line.

Correspondence should be addressed to Dr. Cynthia A. Lemere, Center for Neurological Diseases, Harvard New Research Building, Room 636F, 77 Avenue Louis Pasteur, Boston, MA 02115. E-mail: clemere@rics.bwh.harvard.edu.

DOI:10.1523/JNEUROSCI.0381-06.2006

 0270-6474/06/264717-12$15.00/0

Active immunization induces both a humoral (antibody mediated) and cellular immune response (via T lymphocytes). In AD mouse models, peripheral injection of Aβ-specific antibodies (i.e., passive immunization) reduced cerebral Aβ levels (Bard et al., 2000; DeMattos et al., 2001) and improved cognitive function (Dodart et al., 2002) but also led to microhemorrhages in aged APP-tg mice with abundant vascular amyloid (Pfeifer et al., 2002; Wilcock et al., 2004b; Racke et al., 2005).

The majority of anti-Aβ antibodies generated in mice (Lemere et al., 2000; Town et al., 2001; McLaurin et al., 2002; Cribbs et al., 2003), monkeys (Lemere et al., 2004), and humans (Lee et al., 2005) recognize an epitope located within the amino terminus of Aβ protein (e.g., Aβ1–15). In humans (Monsonego et al., 2003) and mice (Monsonego et al., 2001; Cribbs et al., 2003), T-cells recognize a more C-terminal epitope (within Aβ 16–42). These observations have been used to design alternative immunogens, which encompass the N-terminal antibody epitope of Aβ but lack the more C-terminal T-cell reactive sites for immunization in AD animal models. Such shorter Aβ fragments have been shown to lead to an immune response when conjugated to T-helper (Th) cell epitopes (Monsonego et al., 2001) and/or have been used on a branched peptide framework (Agadjanyan et al., 2005)

The purpose of this study was to determine the humoral and cellular immune responses in wild-type mice of four alternative Aβ1–15-containing intranasal immunogens in combination with mutant *Escherichia coli* heat-labile enterotoxin LT(R192G), which is an excellent adjuvant for mucosal immunization (Dickinson and Clements, 1995; Lemere et al., 2002) and currently in phase I clinical trials (www.clinicaltrials.gov, NIH). In addition, we tested the ability of two immunogens to ameliorate Aβ pathology and one immunogen to improve behavioral deficits in human APP familial AD ($hAPP_{FAD}$) mice (J20 line) (Mucke et al., 2000), an AD animal model.

Materials and Methods

Peptides and CD spectroscopy. Immunogens [DAEFRHDSGYEVHHQ-KK-DAEFRHDSGYEVHHQ (2×Aβ1–15), RGD (Arg-Gly-Asp)-2×Aβ1–15 (R-2×Aβ1–15), KQIINMWQAVGKAMYA-KK-DAEFRHDSGYEVHHQ (T1-Aβ1–15), T1-RGD-KK-Aβ1–15 (T1-R-Aβ1–15) (Alpha Diagnostics, San Antonio, TX), and human Aβ1–40 and Aβ1–42 peptide (Dr. D. Teplow, Biopolymer Laboratory, Center for Neurologic Diseases, Boston, MA)] were dissolved directly in distilled water at 4 mg/ml. Only the Aβ1–40 plus Aβ1–42 peptides (Aβ40/42: 3 mg/ml Aβ1–40 and 1 mg/ml Aβ1–42) were incubated overnight at 37°C. Circular dichroism (CD) spectra of the peptides were recorded on an Aviv model 62A DS spectropolarimeter (Aviv Associates, Lakewood, NJ) using quartz cuvettes of 0.1 cm path length. All spectra were recorded at 25°C over a wavelength range of 195–260 nm. Qualitative secondary structure assignments were done as described previously (Johnson, 1990).

Animals and treatments. Immunization experiments were performed in 6–8 week old, male B6D2F1 wild-type mice (Taconic Farms, Germantown, NY; $n = 4$ mice per group) or $hAPP_{FAD}$ [J20 line; neuronal expression of familial-AD mutant hAPP: K670N, M671L, V717F, under the PDGFβ promoter (Mucke et al., 2000)] animals on a mixed C57BL/6 and DBA2 (B6D2) background ($n = 6$ 6-month-old mice for R-2×Aβ1–15, $n = 6$ for corresponding control; $n = 6$ 4.5-month-old mice for 2×Aβ1–15, $n = 7$ for control; gender-balanced with a maximal age difference between individual animals <1 month per treatment). All animal use was approved by the Harvard Standing Committee for Animal Use and was in compliance with all state and federal regulations. The mucosal adjuvant, mutant *E. coli* heat-labile enterotoxin LT(R192G) (gift from J. Clements, Tulane University School of Medicine, New Orleans, LA) was reconstituted with distilled water and mixed with an aliquot of the peptides just before use. Peptide plus LT(R192G) intranasally immunized mice received, on the same day, two doses of 25 μg immunogen-peptide plus 2.5 μg LT(R192G) (in a total volume of 9 μl) to the naris as described previously (Maier et al., 2005b).

Plasma and tissue collection. Blood plasma was collected from the tail as described previously (Maier et al., 2005b). One week after the final immunization, mice were killed by CO_2 inhalation and transcardially perfused with PBS. The brain was removed and divided sagittally. One hemibrain was fixed for 2 h in 10% buffered formalin while the other hemibrain was snap frozen in liquid nitrogen for biochemical analysis. Hemibrain, liver, kidney, and snout tissues were embedded in paraffin as described previously (Lemere et al., 2003; Maier et al., 2005b). TBS-soluble and 5 M guanidinium-soluble (i.e., TBS insoluble) brain homogenates were prepared as reported previously (Weiner et al., 2000).

Anti-Aβ antibody ELISA and Aβ ELISA. Anti-Aβ40 antibodies in mouse plasma were measured as described previously with an anti-Aβ40 antibody ELISA (Lemere et al., 2002). ELISAs for antibody isotypes and epitope-mapping were performed as reported previously (Maier et al., 2005b) with two differences. First, biotin-anti-mouse-IgG2a (Serotec, Raleigh, NC) was used as a secondary antibody for detection of IgG2a antibodies and, second, epitope mapping ELISA plates were coated with the same peptide (2 μg/ml in 50 mM carbonate buffer, pH9.6) used for immunizing the mice. Briefly, for epitope-mapping, dilutions of mouse plasma (depending on concentration of antibodies between 16,000 and 256,000) were absorbed overnight with the same concentration (35 μg/ml) of Aβ1–15, Aβ1–7, Aβ3–9, Aβ7–12, Aβ11–25, Aβ26–42, Aβ1–42 [Center for Neurological Diseases (CND), Biopolymer Laboratory], a three-amino-acid peptide RGD (Peninsula Laboratories, San Carlos, CA), the RGD-motif containing protein fibronectin (Sigma-Aldrich, St. Louis, MO), or the different immunogens peptides. The remaining ability of the antibodies to bind plate-bound immunogen was then measured by ELISA.

Aβ levels were measured in plasma using an $Aβ_{x-total}$ ELISA as described previously (Weiner et al., 2000). Aβ40 and Aβ42 levels were measured in brain homogenates by ELISA as described previously (Levites et al., 2006).

Splenocyte proliferation assay and detection of cytokines. Spleens were pooled for wild-type B6D2F1 mice immunized with the same immunogen, whereas splenocytes from $hAPP_{FAD}$ mice were isolated, cultured, and restimulated individually as described previously (Maier et al., 2005b). The same peptides used for immunization were used for restimulation. A stimulation index (SI) was calculated using the following formula: counts per minute (CPM) of well with peptide antigen/CPM with no antigen. Stimulation with concavalin A was used to ensure the viability of the cells and the average stimulation indices were similar in all groups analyzed (data not shown).

Immunohistochemistry. Ten micron paraffin sections of human AD brain, mouse brain, liver, kidney, and snouts were mounted on glass slides and immunohistochemistry was performed as reported previously (Lemere et al., 2002) using Vector Elite ABC kits (Vector Laboratories, Burlingame, CA). The following antibodies were used for neuropathological analysis: anti-CD45 (1:5000; Serotec), anti-GFAP (1:500; Dako, Carpinteria, CA), anti-CD5 (1:200; BD PharMingen, San Jose, CA), rabbit polyclonal anti-Aβ R1282 (1:1000; gift from D. Selkoe, CND, Boston, MA) and anti-Aβ40 and anti-Aβ42 (1:500; BioSource, Camarillo CA). For quantification of immunoreactivity, acquisition of images was performed in a single session using a QICAM camera (Qimaging, Burnaby, British Columbia, Canada) mounted on an Olympus (Melville, NY) BX50 microscope, with threshold of detection held constant during analysis. The percent area occupied by immunoreactivity was calculated for 3–4 equidistant sections of hippocampus per animal. Computer-assisted image analysis was performed on images of the hippocampus using IP Lab Spectrum (Fairfax, VA) 3.1 image analyzer. Thioflavine S staining for fibrillar Aβ was performed by incubating slides in a 1% aqueous solution of Thioflavine S for 10 min followed by rinses in 80 and 95% ethanol, and then distilled water. The Perl's Prussian blue method was used to visualize ferric iron in hemosiderin as a measure for hemorrhages (Pfeifer et al., 2002). Mouse plasma, diluted 1:1000, 1:10,000, and 1:25,000 was used for immunohistochemistry (IHC) on formic acid-pretreated, formalin

fixed, human AD brain sections or on nonfixed, non-pretreated 10 μM human AD brain cryosections (Racke et al., 2005).

Behavioral testing. The effect of immunization on cognition was evaluated in the spatial reference memory version of the Morris water maze (MWM). Two series of tests were administered to evaluate acquisition and learning reversal of spatial information. All MWM tests were performed in a pool 160 cm in diameter, with an escape platform submerged 1 cm under the water (11 cm in diameter). The surface of the water (20–21°C) in the pool was made opaque by the addition of small white plastic beads (Cain et al., 1997). The pool was situated in a testing room fitted with several distant spatial cues (posters on black curtain). The first test was performed over 12 d, with the escape platform located 30 cm from the wall of the pool in quadrants 1 or 3 (counter-balanced for one-half of mice in each tested group). Each mouse was given four daily 90 s training trials with intertrial intervals between 30 and 50 min. During each trial, a mouse was released into the water facing the wall of the pool from semirandomly chosen cardinal compass points (north, east, south, and west). To evaluate the development of spatial memory, all mice were given probe trials on days 2, 6, and 12 of training. During probe trials, which were administered as the first trial of the day, the escape platform was removed from the pool and the mice were allowed to search the pool uninterrupted for 60 s. The second series of reference memory MWM tests addressed the plasticity of learning reversal in the mice. We used a 5 d paradigm of six daily trials (90 s maximum) with 3 d of initial acquisition [the escape platform located in a balanced way in quadrants 2 (for one-half of the mice) or 4 (for another one-half; 50 cm from the wall], and 2 d with reversed platform location (in quadrants 4 and 2, 35 cm from the wall). Varying the distance of the platform location from the wall during each learning acquisition prevented the mice from using nonspatial, chaining strategy during navigation (Janus, 2004). Spatial memory was evaluated in 60 s probe trials administered 1 h after the last training trial on days 3 and 5.

Each reference-memory test was followed by a cued (visible platform) version of MWM (4 trials/d, 2 d) in which an escape platform was marked by a 15-cm-high red post with a yellow/black ball, and the extra-maze cues (posters) were removed from the black curtain surrounding the pool. The swim path of a mouse during each trial was recorded by a video camera suspended 2 m above the center of the pool and connected to a video tracking system (Advanced Tracker VP200; Hampton Video Systems Image, Buckingham, UK) and a personal computer running Hampton Video Systems software.

Data analysis. The scores of each mouse were averaged across four (or six for the reversal experiment) daily training trials in both cued and conventional reference-memory MWM tests. The following variables characterizing the performances of mice in the water maze were chosen for analysis: latency time (seconds) it took a mouse to reach and climb the platform, and the length of swim path (centimeters). In most cases, the latency and the path length were highly positively correlated, therefore only the path was reported. The locomotor activity of the mice was analyzed using an average swim speed (meters/second, excluding bouts of inactivity or floating) and was very similar between both groups in all tests (data not shown). The spatial memory for the platform location during probe trials was evaluated by the analysis of the dwelling time in each quadrant of the pool, and the analysis of an annulus-crossing index (ACI). The ACI represents the number of crosses over the platform site in a quadrant that contained the escape platform [target quadrant (TQ)] adjusted for crosses over platform sites in alternative quadrants (i.e., ACI equals the number of site crosses in the TQ minus an average of crosses of sites in the other three quadrants of the pool).

A factorial model ANOVA (Prism software; GraphPad, San Diego, CA) was used with the treatment as a between-subject factor, and training days as a within-subject (repeated measure) factor. A Spearman correlation was used to correlate average antibody titers developed by mice during the immunization period (week 20–30) with spatial memory indices (ACI) obtained during two probe trials applied in the series of learning-reversal tests. Based on the previously obtained results, which demonstrated a beneficial effect of immunization on learning and memory in mice (Janus et al., 2000; Morgan et al., 2000, Sigurdsson et al., 2004, Jensen et al., 2005), we adopted a directional, one-tailed test while evaluating the association between the titer levels and memory indices. A Mann–Whitney *U* (MWU) test was used for statistical analysis of ACI and percentage dwelling time values from probe trials, as well as for immunoreactive area and Aβ levels in $hAPP_{FAD}$-tg mice determined by ELISA. The critical α level was set to 0.05 for all statistical analyses. All values reported are average ± SEM.

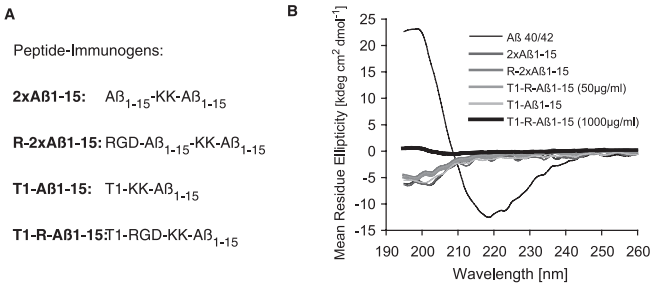

Figure 1. Design and biophysical characterization of four novel peptide immunogens containing the first 15 amino acids (Aβ1–15) of full-length Aβ1–42. ***A***, The first two novel immunogens consist of a tandem repeat of the Aβ1–15 sequence linked by two lysines with (R-2×Aβ1–15) or without (2×Aβ1–15) the addition of a three-amino-acid RGD-motif at the N terminus of the peptide. The third and fourth immunogens contain a previously characterized cross-species active T1 Th cell epitope connected by two lysines to the Aβ1–15 sequence with (T1-R-Aβ1–15) or without (T1-Aβ1–15) the RGD motif N-terminal to the lysine linker. ***B***, CD spectra of the four novel peptides and Aβ40/42. Aβ40/42 shows a typical β-sheet spectrum characterized by a minimum near 220 nm and a maximum near 195 nm (thin black line). The four novel immunogen-peptides exhibit spectra indicative of unstructured peptides (gray lines) that are independent of the peptide concentration, except for T1-R-Aβ1–15, which shows trace amounts of helical content at 1000 μg/ml (thick black line; minima at 208 and 222 nm, maximum at 198 nm).

Results

Design and biophysical characterization of four novel Aβ1–15-containing peptide-immunogens

The first novel immunogen consisted of a tandem repeat of the human N-terminal Aβ1–15 sequence linked by two lysines (2×Aβ1–15) (Fig. 1*A*) to reduce the production of antibodies against newly created epitopes created by the direct linkage of a tandem repeat (Oishi et al., 2001). R-2×Aβ1–15 peptide, the second immunogen, contained, in addition, a three-amino-acid RGD-cell attachment motif at the N terminus, which was previously shown to increase immunogenicity and replace the use of adjuvant in combination with a different immunogen (Yano et al., 2003). The third immunogen contained a previously characterized, exogenous T1 T-helper cell epitope connected by two lysines to a single Aβ1–15 sequence (T1-Aβ1–15). The T1 sequence is a T-cell epitope of HIVIIIB gp120 (human immunodeficiency virus type IIIB envelope glycoprotein 120) (Cease et al., 1987) mutated to enhance immunogenicity and is recognized at multiple major histocompatibility complex (MHC) loci in mice (Ahlers et al., 1997) and other species such as goats, nonhuman primates, and humans (Hart et al., 1990; Haynes et al., 1993; Yano et al., 2003). The fourth immunogen was T1-R-Aβ1–15 and included the RGD motif N terminal to the lysine linker, which was the most efficient position according to a previous study (Yano et al., 2003).

As a first step, we determined whether 2×Aβ1–15, R-2×Aβ1–15, T1-Aβ1–15, and T1-R-Aβ1–15 aggregate into a β-sheet structure as has been observed for full-length Aβ and its C-terminal fragments. At a peptide concentration of 50 μg/ml, all four novel immunogen peptides showed a CD spectrum typical for an unstructured peptide, whereas Aβ40/42 showed a spectrum characteristic for β-sheet structures (minimum near 220 nm, maximum near 195 nm) (Fig. 1*B*, thin black line). This was

similar at the higher concentration of 1 mg/ml, except for T1-R-Aβ1–15 peptide, which showed trace amounts of helical content (minima at 208 and 222 nm, maximum at 198 nm) (Fig. 1*B*, thick black line). This is in agreement with previous observations, suggesting a potential for the T-cell site T1 to form amphipathic helices (Cease et al., 1987). Thus, our four novel immunogens did not form β-sheet aggregates and, consequently, are unlikely to present potential neoepitopes specific for aggregated Aβ.

Characterization of anti-Aβ antibody responses in nontransgenic mice

In the first set of experiments, B6D2F1 wild-type mice were intranasally immunized once a week with 50 μg of 2×Aβ1–15 or R-2×Aβ1–15 and 5 μg of LT(R192G) adjuvant. Every two weeks, blood plasma was collected and anti-Aβ antibody levels were determined by anti-Aβ40 ELISA (Fig. 2*A*). After 4 weeks, low levels of anti-Aβ antibodies could be detected in all four animals immunized with R-2×Aβ1–15 and in two of four animals immunized with 2×Aβ1–15. In the following weeks, anti-Aβ antibody levels for the R-2×Aβ1–15 immunogen continued to increase faster and peaked at 1884 ± 170 μg/ml by week 8 and slightly dropped thereafter. Antibody levels for 2×Aβ1–15 reached 1002 ± 194 μg/ml by week 8 and remained at this high level after additional treatments. Antibody levels for both immunogens were comparable after week 12 and were overall ~2–3 times higher compared with immunization with aggregated Aβ40/42 (Fig. 2*B*). Immunization with these peptides in the absence of an adjuvant, or immunization with adjuvant alone, did not induce detectable levels of antibodies (Maier et al., 2005a).

In a second set of experiments, we compared intranasal immunization using 50 μg T1-R-Aβ1–15, T1-Aβ1–15, or Aβ40/42 and 5 μg LT(R192G) in B6D2F1 mice. After six weeks, three of four animals produced low levels of antibodies increasing up to 252 ± 127 μg/ml by week 12 with the T1-R-Aβ1–15 peptide. T1-Aβ1–15-immunized animals had detectable antibody levels by week 8, increasing up to 333 ± 102 μg/ml by week 12. Overall, antibody titers induced by T1 containing-immunogens remained approximately two times lower compared with those mice immunized with full-length Aβ40/42. Immunization with T1-R-Aβ1–15 or T1-Aβ1–15 in the absence of adjuvant induced only very low antibody levels (Fig. 2*B*) in a subset of animals. No anti-Aβ antibodies were detected in preimmune plasma from any mouse included in these studies.

Isotypic profiles and mapping of antibody epitopes

Ig isotyping of anti-Aβ antibodies was performed on the final bleed using isotype-specific ELISAs. IgG2b, a noninflammatory Th2 isotype Ig, was the predominant Ig isotype in all five treatment groups. In addition, lower levels of IgG1 (Th2) and IgG2a (Th1) were detected in all groups, whereas low amounts of IgA and IgM were detected in the R-2×Aβ1–15- and 2×Aβ1–15-immunized groups (for overview, see Fig. 3*A*, Table 1).

To determine the specificity of the Aβ-antibodies, three different plasma dilutions (1:1000, 1:10,000, and 1:25,000) from each of the immunized mice were used for IHC on human AD cortical brain sections. Antibodies induced by all five immunogens labeled diffuse and compacted plaques similar to the monoclonal anti-Aβ antibody 6E10 raised against Aβ1–17 (Fig. 3*D*). Representative examples are shown for plasma from 2×Aβ1–15- (Fig. 3*B*) and T1-R-Aβ1–15-immunized (Fig. 3*C*) animals. Overall, the highest plasma dilution able to stain plaques in IHC correlated well with the antibody titers determined by anti-Aβ40 ELISA (data not shown).

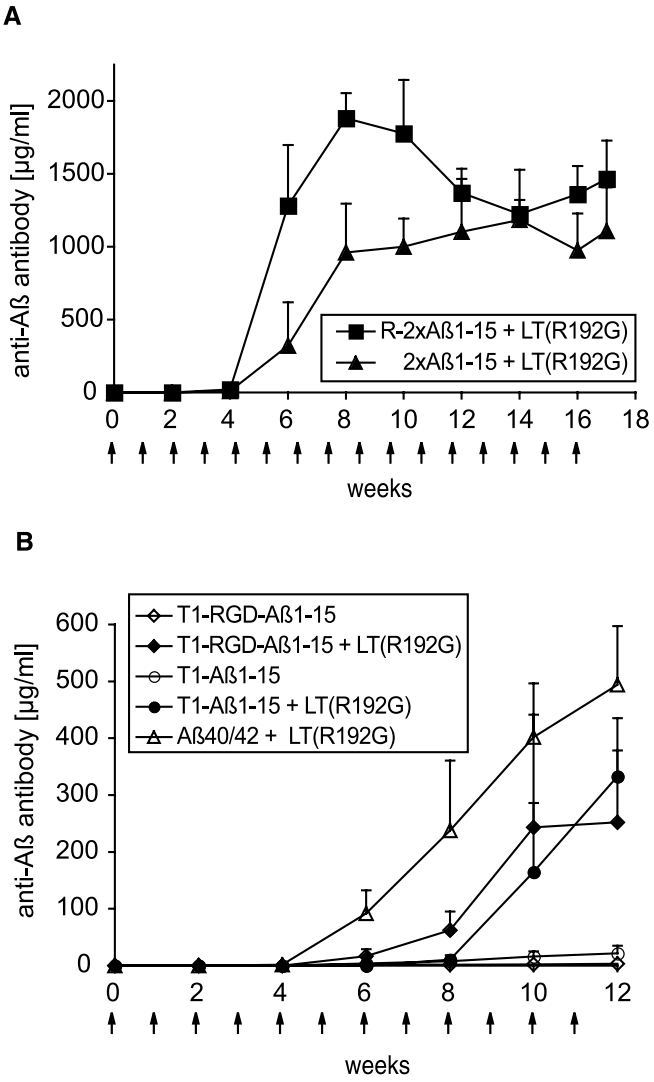

Figure 2. Plasma anti-Aβ antibody levels after weekly, intranasal immunization of B6D2F1 mice with 50 μg of peptide plus 5 μg of mutant, heat-labile enterotoxin LT(R192G) adjuvant as determined by anti-Aβ40 ELISA. ***A***, Immunization with 2×Aβ1–15-containing immunogens generated high serum titers of anti-Aβ antibodies after six weeks. R-2×Aβ1–15 plus LT(R192G)-immunized animals showed a faster increase in their antibody levels than 2×Aβ1–15 plus LT(R192G)-immunized mice but reached similar levels after 12 weeks and were ~2–3 times higher compared with immunization with Aβ40/42 (***B***). ***B***, Weekly immunization with T1-R-Aβ1–15 or T1-Aβ1–15 plus LT(R192G) led to the generation of intermediate antibody levels, which remained below the titers achieved with Aβ40/42 plus LT(R192G) immunization. In the absence of adjuvants, T1-containing peptides induced only very low antibody levels. Data are mean ± SEM for each group ($n = 4$). Arrows indicate intranasal dosing schedule.

Preincubation with Aβ1–15, Aβ1–7, and to a lesser extent Aβ3–9 inhibited binding of antibodies from 2×Aβ1–15- or R-2×Aβ1–15-immunized animals to immunogen-peptide-coated ELISA plates, indicating that the major antibody epitope is found within Aβ1–7 (Fig. 3*E*). In T1-Aβ1–15- or T1-R-Aβ1–15-immunized animals, Aβ1–15 reduced antibody binding similar to full-length immunogen or Aβ1–42. Absorption with shorter Aβ1–7 or Aβ3–9 reduced the OD less compared with antibodies of 2×Aβ1–15- or R-2×Aβ1–15-immunized animals, indicating that the major antibody epitopes are found within Aβ1–15 with the T1-containing immunogens. Aβ1–42 had a similar absorbing effect compared with the immunogen peptides themselves, and the addition of RGD peptide or the RGD-containing protein

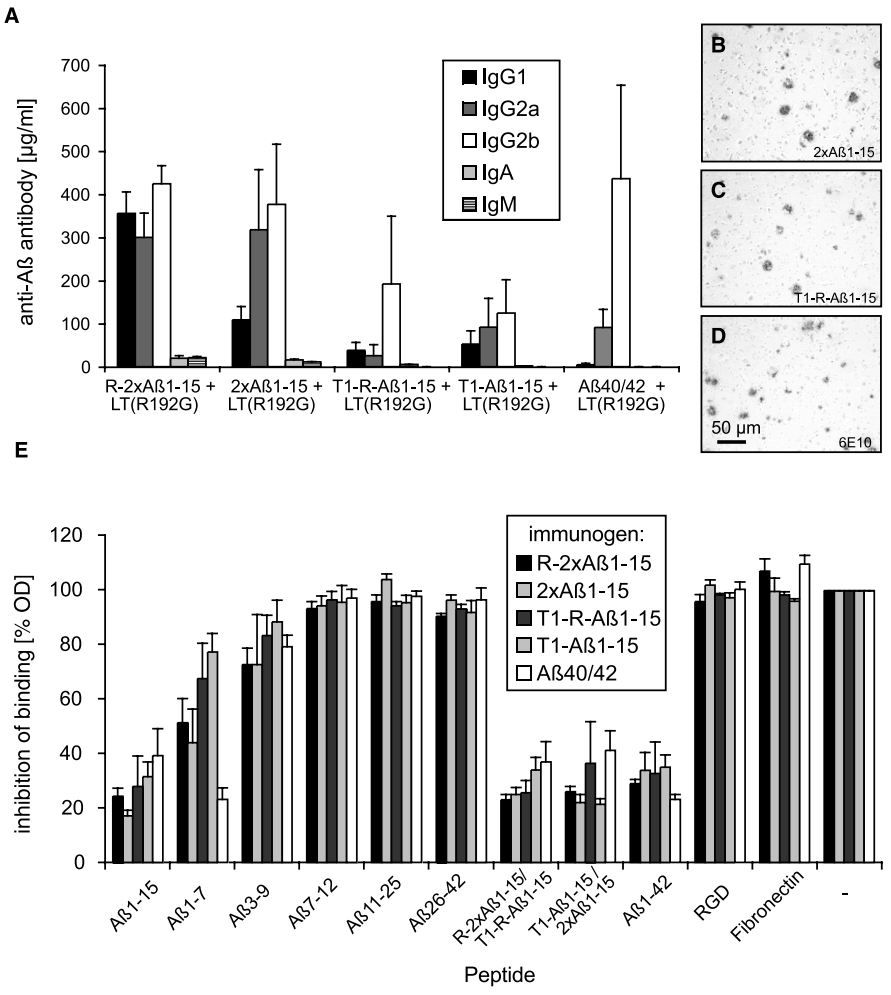

Figure 3. Immunoglobulin isotyping of plasma IgG1, IgG2a, IgG2b, IgA, and IgM anti-Aβ antibodies as determined by isotype-specific ELISA in the final bleed. ***A***, IgG2b anti-Aβ antibodies were the predominant Ig isotype in all five treatment groups. In addition to IgG2b antibodies, mice immunized with R-2×Aβ1–15 or 2×Aβ1–15 produced high levels of IgG2a and IgG1, and mice immunized with T1-Aβ1–15 or Aβ40/42 showed intermediate levels of mainly IgG2a. Low levels of IgA and IgM antibodies were present in mice immunized with R-2×Aβ1–15 and 2×Aβ1–15. Data are mean ± SEM. ***B–D***, Antibodies induced by all four novel immunogens were able to detect diffuse and compacted plaques on formalin-fixed paraffin-embedded brain tissue from AD patients similar to anti-Aβ antibody 6E10 (***D***). A representative example is shown for a 1:10,000 dilution of plasma from a 2×Aβ1–15- (***B***) or T1-R-Aβ1–15-immunized (***C***) animal. ***E***, Epitope-mapping of antibodies was performed by preincubating mouse plasma overnight with short Aβ peptide fragments. The remaining ability of the antibodies to bind plate-bound immunogen was then measured by ELISA. Preincubation with Aβ1–15, Aβ1–7, and to a lesser extent Aβ3–9 inhibited binding to plate-bound immunogen, indicating that the major antibody epitope is within Aβ1–15 for mice immunized with T1-Aβ1–15 or T1-R-Aβ1–15 and within Aβ1–7 for mice immunized with 2×Aβ1–15 or R-2×Aβ1–15. The immunogen peptides or Aβ1–42 reduced the OD to a similar extent compared with Aβ1–15, and the addition of the RGD peptide or the RGD-containing protein fibronectin did not interfere with binding of the antibodies in the assay. This indicates that the vast majority of antibodies were directed against the Aβ1–15 sequence and not against other parts of the immunogen peptides. OD levels are shown relative to no peptide control. Data are mean ± SEM ($n = 4$).

fibronectin did not interfere with binding of the antibodies to their immunogen peptide. This confirmed the specificity of the antibodies to the N-terminal Aβ sequence and excludes a major population of antibodies directed against other sequences of the immunogen peptides.

Strong cellular immune response against the immunogen in the absence of specific proliferation against full-length Aβ

To characterize the cellular immune response, splenocyte cultures were established from R-2×Aβ1–15- or 2×Aβ1–15- (Fig. 4*A–D*) and T1-R-Aβ1–15-, T1-Aβ1–15-, or Aβ40/42-immunized (Fig. 4*E–H*) wild-type mice and stimulated with different concentrations of the immunogen peptides Aβ40/42 or Aβ1–15 (Fig. 4). Highest SIs were observed in splenocytes restimulated with their corresponding immunogen (Fig. 4*A*,*B*,*E–G*). A strong, cross-reactive proliferative response was also detected if splenocytes were restimulated with the corresponding immunogen containing or lacking the RGD-motif. For example, splenocytes from R-2×Aβ1–15-immunized animals showed an intermediate, cross-reactive proliferative response after restimulation with 2×Aβ1–15, and vice versa (Fig. 4*A*,*B*). To determine whether the cellular immune response was directed to Aβ, we restimulated splenocytes from all groups with aggregated full-length Aβ40/42. This induced proliferation only in Aβ40/42-immunized animals, as expected from previous studies (Seabrook et al., 2004; Maier et al., 2005b), but did not induce significant SI in other immunized groups (Fig. 4*C*,*G*). After restimulation with the highest dose of Aβ40/42 (50 µg/ml), very low proliferation was detected in splenocytes of R-2×Aβ1–15- and 2×Aβ1–15-immunized mice, but a comparable SI was also found in nontreated animals (SIs of 4.3, 5.7, and 2.1, respectively) (Fig. 4*C*), indicating that this may have been caused by a general stimulation by peptide aggregates. No significant responses were detected after restimulation with Aβ1–15 in any group of animals (Fig. 4*D*,*H*).

High antibody titers and an immunogen-specific cellular immune response in R-2×Aβ1–15- or 2×Aβ1–15-immunized $hAPP_{FAD}$ mice

Because R-2×Aβ1–15 and 2×Aβ1–15 immunogens induced high titers of specific anti-Aβ antibodies in B6D2F1 wild-type mice, we tested the ability of these peptides to induce an immune response and their efficacy to reduce cerebral Aβ burden in $hAPP_{FAD}$ transgenic mice (line J20) (Mucke et al., 2000). In the first experiment, $hAPP_{FAD}$ mice were immunized intranasally with R-2×Aβ1–15 plus LT(R192G) adjuvant weekly starting at 6 months of age, when plaque deposition was in early stages. The control group received adjuvant only. Within 6–8 weeks of treatment, R-2×Aβ1–15-immunized mice developed high antibody titers, which peaked at 1173 ± 341 µg/ml at week 14 and decreased slightly after we switched to biweekly intranasal treatment (Fig. 5*A*). The main immunoglobulin isotypes in plasma from the final bleed were IgG2b and IgG1 (both noninflammatory Th2 immunoglobulins) (Fig. 5*B*), with proportionally less IgG2a (proinflammatory Th1) compared with levels detected in wild-type mice. Low levels of IgA and IgM were detected in mice immunized with R-2×Aβ1–15. The antibodies recognized epitopes within Aβ1–15 and Aβ1–7 as described earlier for

Table 1. Summary results of all immunization experiments

Genotype	Immunogen	Antibody titers[a]	Relative levels of Ig isot/pos[b]					Epitope[b]	Histology hippocampus [% change[c]]						Brain [% change[c]]				Plasma [% change[c]]		
			IgG1	IgG2a	IgG2b	IgA	IgM		$A\beta_{tot}$	$A\beta_{42}$	$A\beta_{40}$	Thio S	CD45	GFAP	Gx[d] $A\beta_{42}$	Gx[d] $A\beta_{40}$	TBS[e] $A\beta_{42}$	TBS[e] $A\beta_{40}$	$A\beta_{tot}$	$A\beta_{42}$	$A\beta_{40}$
WT B6D2F1	R-2xAβ1-15	1372 ± 165	+++	+++	+++	+	+	$A\beta_{1-7}$													
	2xAβ1-15	1103 ± 363	++	+++	+++	+	+	$A\beta_{1-7}$													
	T1-RAβ1-15	252 ± 127	+	+	+++	−	−	$A\beta_{1-15}$													
	T1-Aβ1-15	333 ± 102	+	++	+++	−	−	$A\beta_{1-15}$													
	Aβ1-40/42	532 ± 101	−	+	+++	−	−	$A\beta_{1-7}$													
$hAPP_{SW}$ (J20)	R-2xAβ1-15	931 ± 183	++	+	+++	++	++	$A\beta_{1-7}$	−74*	−74*	−54*	−54*	−18	−18	−35	−36	+48*	+51*	+61*	nd	nd
	2xAβ1-15	1685 ± 483	++	+	+++	+	+	$A\beta_{1-7}$	−73*	−70*	−6	+4	+45	+9	−34	−2	−10	−9	nd	+330*	+85*

[a]bleed week 12 (μg/ml).

[b]Final bleed: ELISA.

[c]Compared with corresponding control.

[d]Gx:TBS insoluble Aβ (5 M guanidinium-soluble).

[e]TBS-soluble Aβ.

nd, Not determined.

*Significant difference compared with control (P 0.05, MWU).

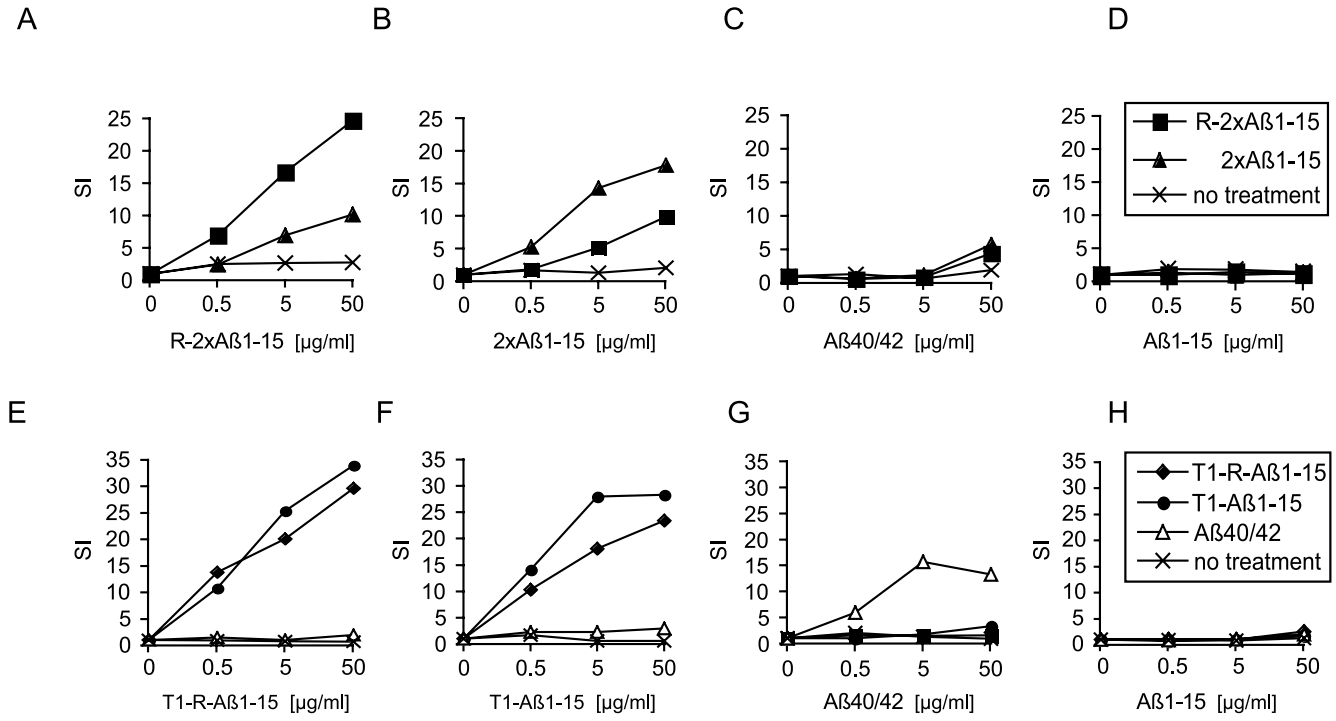

Figure 4. Splenocytes from 2×Aβ1–15- or R-2×Aβ1–15- (***A–D***) and T1-Aβ1–15-, T1-R-Aβ1–15-, or Aβ40/42-immunized (***E–H***) animals were isolated and cultured as indicated in the presence of 0, 0.5, 5, or 50 μg/ml R-2×-Aβ1–15 (***A***), 2×Aβ1–15 (***B***), T1-R-Aβ1–15 (***E***), T1-Aβ1–15 (***F***), Aβ40/42 (***C***, ***G***), and Aβ1–15 (***D***, ***H***) for 72 h, after which [^{3}H] thymidine was added for 18 h. The CPM was determined and an SI calculated. Splenocytes isolated from immunized mice showed a high SI in response to stimulation with their immunogen peptide. In splenocyte cultures of animals immunized with the novel peptide immunogens, only very low and mainly nonspecific proliferation was observed after restimulation with the highest dose of Aβ40/42 (***C***, ***G***). No proliferation was detected in response to Aβ1–15 (***D***, ***H***).

B6D2F1 mice (data not shown). No antibodies were detected in plasma of control animals.

After 24 weeks of treatment, splenocytes of 12-month-old $hAPP_{FAD}$ mice were isolated and restimulated with R-2×Aβ1–15, Aβ40/42, or Aβ1–15. Comparable with wild-type mice, intermediate SIs were detected after restimulation with R-2×Aβ1–15 (Fig. 5*C*), but only very low SIs were measured after restimulation with the highest concentration of aggregated full-length Aβ40/42 (Fig. 5*D*), with similar values for immunized and control animals, indicating a lack of cellular immune response to full-length Aβ. No significant SIs were detected for restimulation with the same concentrations of Aβ1–15, fibronectin, or RGD-motif-containing protein (SI <2; data not shown).

In a second experiment, we started immunization at an age of 4.5 months, just before plaque deposition, with 2×Aβ1–15 plus LT(R192G) or adjuvant only in the control group. Antibody titers peaked after 12 weeks of immunization with an average of 1686 ± 483 μg/ml (Fig. 5*A*) and had Ig isotypes and antibody epitopes similar to those observed after immunization with R-2×Aβ1–15 (Fig. 5*B*). After 30 weeks of treatment, splenocytes of these 12-month-old $hAPP_{FAD}$ mice were isolated and restimulated with 2×Aβ1–15, Aβ1–40, Aβ40/42, or Aβ1–15. Intermediate stimulation indices were detected after restimulation with 2×Aβ1–15 (Fig. 5*E*), whereas no specific proliferation was observed after restimulation with Aβ1–40 (Fig. 5*F*), aggregated Aβ40/42, or Aβ1–15 (data not shown).

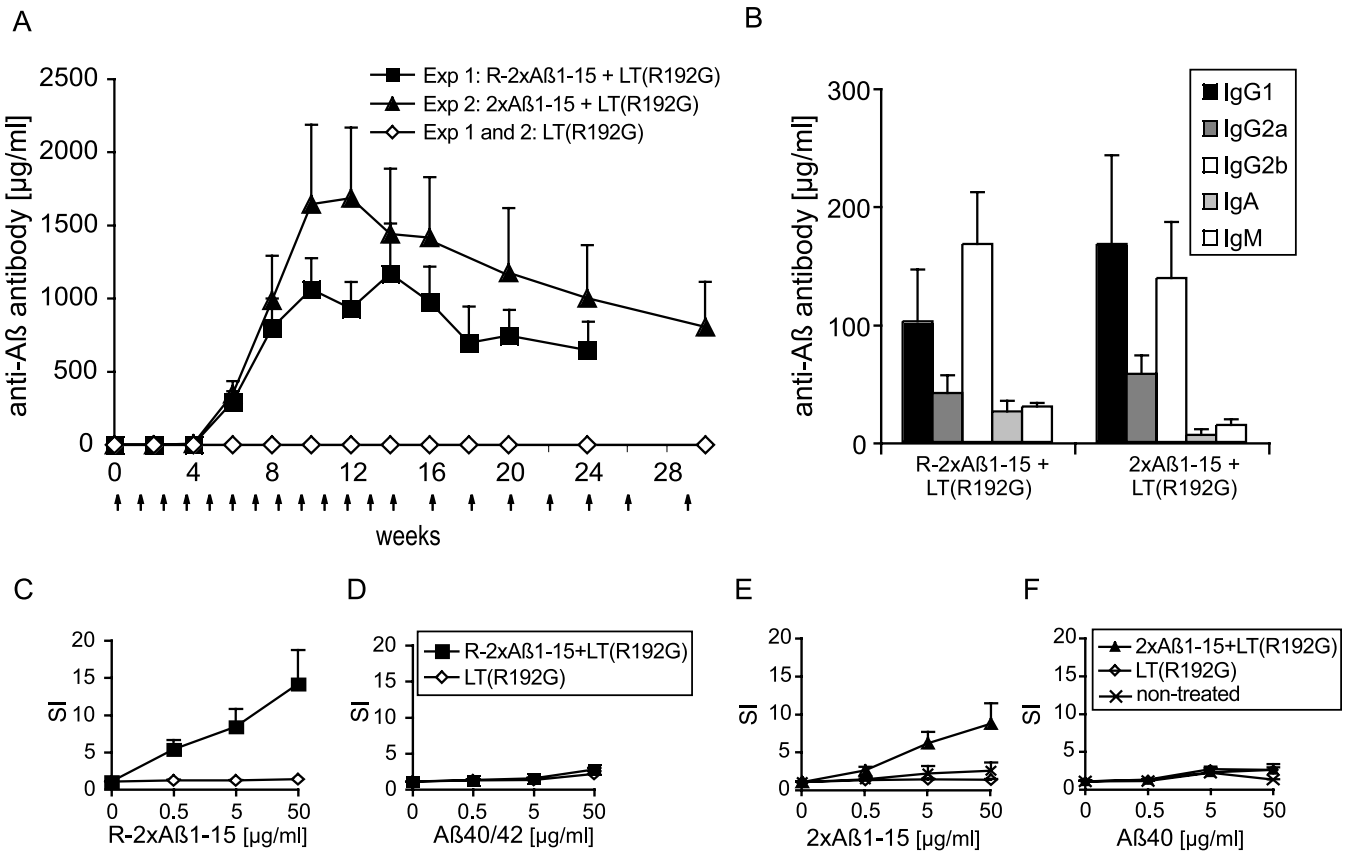

Figure 5. ***A***, Immunization of $hAPP_{FAD}$ (J20 line) animals with R-2×Aβ1–15 ($n = 6$) or 2×Aβ1–15 ($n = 6$) induced high levels of anti-Aβ antibodies as determined by anti-Aβ40 ELISA. Levels peaked at 10–14 weeks and dropped slightly after switching to biweekly immunization after week 14. Arrows indicate the intranasal dosing schedule. ***B***, IgG2b and IgG1 were the main immunoglobulin isotypes of anti-Aβ antibodies in the final bleed of R-2×Aβ1–15- and 2×Aβ1–15-immunized animals. Lower levels of IgA and IgM were detected after immunization with R-2×Aβ1–15. ***C***, Splenocytes from R-2×Aβ1–15 (***C***, ***D***) or 2×-Aβ1–15-immunized (***E***, ***F***) $hAPP_{FAD}$ animals showed intermediate stimulation indices after restimulation with R-2×Aβ1–15 (***C***) and 2×Aβ1–15 (***E***), respectively. Very low, nonspecific proliferation was detected in splenocytes of immunized and LT(R192G)-adjuvant-treated control $hAPP_{FAD}$ mice ($n = 6$ and $n = 7$, respectively) or nontreated B6D2F1 animals ($n = 3$) after restimulation with aggregated Aβ40/42 (***D***) or with Aβ1–40 (***F***). Data are represented as mean ± SEM.

Reduction of cerebral Aβ load after immunization of $hAPP_{FAD}$ mice

Immunization with R-2×Aβ1–15 plus LT(R192G) or 2×Aβ1–15 plus LT(R192G) significantly ($p < 0.05$) reduced total Aβ plaque burden (Fig. 6*A–C*) in the hippocampus by 74 and 73%, respectively, when examined using computer-assisted image analysis. A significant reduction of 74% in Aβ42-specific immunoreactivity was observed in the hippocampus after immunization with R-2×Aβ1–15 plus LT(R192G) ($p < 0.05$) and of 70% after immunization with 2×Aβ1–15 plus LT(R192G) ($p < 0.05$) (Fig. 6*D*,*E*, Table 1). Aβ40-specific immunoreactivity was significantly reduced by 54% with R-2×Aβ1–15 plus LT(R192G) ($p < 0.05$) but not in mice receiving 2×Aβ1–15 plus LT(R192G). Thioflavine S-positive plaque load was significantly reduced by 54% in mice immunized with R-2×Aβ1–15 plus LT(R192G) ($p < 0.05$) but not in those immunized with 2×Aβ1–15 plus LT(R192G). GFAP, a marker for astrocytes, was reduced by 18% in R-2×Aβ1–15 plus LT(R192G) immunized mice versus controls (6.6 ± 1.0% vs 8.3 ± 1.3%, immunized vs control, respectively; $p > 0.05$) and was slightly increased in 2×Aβ1–15 plus LT(R192G) immunized mice (9.1 ± 1.6% vs 8.2 ± 0.6; $p > 0.05$). CD45 immunoreactivity, a marker for activated microglia, was nonsignificantly reduced by 50% in R-2×Aβ1–15 plus LT(R192G) immunized mice compared with vehicle controls (0.8 ± 0.3% vs 1.7 ± 0.4%, respectively), whereas mice immunized with 2×Aβ1–15 plus LT(R192G) showed a trend for an increase by 45% (1.0 ± 0.3% vs 0.7 ± 0.1%, immunized vs control, respectively). CD-5 positive cells, a marker for T-cells, and hemosiderin staining, a histological staining to detect microhemorrhages (Pfeifer et al., 2002), were not detected in the brain parenchyma (data not shown).

Biochemical analysis of plasma Aβ levels by ELISA showed a significant increase of plasma Aβ levels in the final bleed of the immunized animals (Fig. 6*F*,*G*). Cerebral insoluble (guanidinium buffer-soluble) Aβ42 and Aβ40 levels were reduced by 35% in the R-2×Aβ1–15 immunized group compared with the control group, but the changes did not reach significance because of variability and small group size (Fig. 6*F*). TBS-soluble Aβ40 and Aβ42 levels were significantly elevated by 45 and 51%, respectively ($p < 0.05$), in the R-2×Aβ1–15 immunized group. A nonsignificant 34% reduction of cerebral insoluble Aβ42 was observed in 2×Aβ1–15 immunized mice compared with controls, whereas insoluble Aβ40 levels were similar between the groups (Fig. 6*G*) corresponding well with Aβ40 immunoreactivity on brain sections (Fig. 6*E*). TBS-soluble Aβ40 and Aβ42 were comparable in 2×Aβ1–15 immunized and control groups.

Behavioral analysis of 2×Aβ1–15 immunized $hAPP_{FAD}$ mice

The effect of immunization with 2×Aβ1–15 plus LT(R192G) was assessed in a reference-memory version of the MWM, a hippocampus-dependent learning task (Morris et al., 1982). One 2×Aβ1–15 plus LT(R192G)-treated mouse was excluded from

analysis because of the lack of reliable antibody detection (~2 μg/ml). The body weight of mice at the end of the MWM tests was comparable in both groups (data not shown).

Immunized $hAPP_{FAD}$ animals showed faster learning acquisition during the first four training sessions compared with adjuvant-only treated-control $hAPP_{FAD}$ mice (Fig. 7*A*). However, after day 5, both groups showed comparable performances. Overall, both groups showed a significant improvement in performance over the 12 d training period ($p < 0.001$/d, a within-subject factor) with no significant interaction of treatment by day ($p > 0.2$). The results of the probe trials indicate that both cohorts did not retain a clear memory bias for the platform location 20 h after the last training session on day 2 and day 6, as evaluated by the annulus-crossing index (Fig. 7*A*, insert). The results of the percent of time dwelled in the target quadrant were comparable with the annulus-crossing scores (data not shown). To substantiate the results of faster learning acquisition by the immunized $hAPP_{FAD}$ mice, we focused our attention on the learning plasticity in the tested mice.

To test plasticity of spatial memory acquisition, we subjected the same cohorts of mice to the spatial learning reversal MWM task. Consistent with the results of the first test, the 2×Aβ1–15 plus LT(R192G) immunized $hAPP_{FAD}$ mice showed a trend of faster initial acquisition of the new platform location as compared with control $hAPP_{FAD}$ mice (Fig. 7*B*). During the reversal stage, both cohorts of mice showed a comparable response to the platform displacement (Fig. 7*B*, d4 and d5). The results of the probe trials performed at the end of each acquisition stage showed that the immunized $hAPP_{FAD}$ mice formed a positive memory bias in both probe trials on day d3 (initial relearning) and on day d5 (after learning reversal) (Fig. 7*C*). The control $hAPP_{FAD}$ mice showed a negative ACI, which indicates that they searched for the platform in a different quadrant of the pool. The results of the quadrant dwelling time support this interpretation and indicate that these mice persevered with their search in the original, previous location of the pool (Fig. 7*D*). Moreover, spatial memory, as evaluated by ACI, in both probe trials of the learning reversal experiment correlated positively with antibody titers of immunized mice ($r = 0.78$, $p = 0.051$; $r = 0.62$, $p = 0.088$, respectively; $n = 6$). Although, the p values only bordered the $p = 0.05$ significance level (likely because of a small sample size), the trend of improved memory attributable to higher titer level is clear and consistent across both trials.

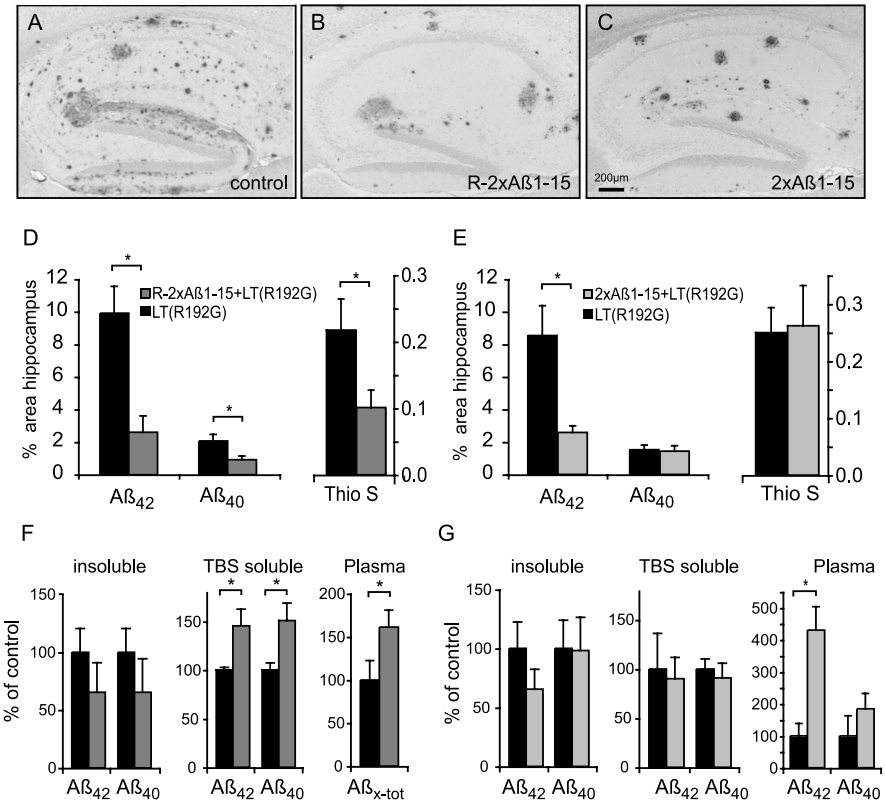

Figure 6. Neuropathological and biochemical analysis of R-2×Aβ1–15- (***B***, ***D***) or 2×-Aβ1–15-immunized (***C***, ***E***) animals compared with their corresponding group of adjuvant-treated control $hAPP_{FAD}$ animals (***A***, ***D***, ***E***). ***A–C***, Sections representing the median Aβ plaque load are shown for each group (***A–C***). ***D***, ***E***, Quantitative image analysis of Aβ42- and Aβ40-specific immunoreactive and Thioflavine S-positive plaque load. Aβ42-, Aβ40-, and Thioflavine S-positive area was significantly reduced in the hippocampus after immunization with R-2×Aβ1–15 plus LT(R192G) (***D***; $p < 0.05$, MWU). 2×Aβ1–15 plus LT(R192G)-immunized mice showed a significant reduction of Aβ42 specific immunoreactivity (***E***; $p < 0.05$, MWU) compared with vehicle treated controls. ***F***, ***G***, Insoluble (guanidinium-soluble) brain Aβ, TBS-soluble brain Aβ, and plasma Aβ levels were analyzed by capture ELISA [absolute values of controls in R-2×Aβ1–15-immunization experiment (***F***): Plasma $Aβ_{x\text{-}tot}$, 0.03 ± 0.01 pmol/ml; Aβ42 insoluble, 2052 ± 417 pmol/g; Aβ40 insoluble, 485 ± 100 pmol/g; Aβ42 TBS soluble, 1.6 ± 0.1 pmol/g; Aβ40 TBS soluble, 0.3 ± 0.1 pmol/g; and in the 2×Aβ1–15-immunization experiment (***G***, measured in a different ELISA run): Aβ40 plasma, 0.9 ± 0.6 pmol/ml; Aβ42 plasma, 0.3 ± 0.1 pmol/ml; Aβ42 insoluble, 3590 ± 800 pmol/g; Aβ40 insoluble, 132 ± 32.5 pmol/g; Aβ42 TBS soluble, 2.1 ± 0.8 pmol/g; Aβ40 TBS soluble, 4.6 ± 0.5 pmol/g]. Asterisk indicates a significant difference (MWU, $p < 0.05$). Data are represented as mean ± SEM.

Discussion

We tested four novel immunogens encompassing either a tandem repeat of two lysine-linked Aβ1–15 sequences (2×Aβ1–15) or Aβ1–15 synthesized to a cross-species active T1 T-helper cell epitope (T1-Aβ1–15) and each with the addition of a three-amino-acid RGD-cell attachment motif (R-2×Aβ1–15; T1-R-Aβ1–15). Intranasal immunization of B6D2F1 wild-type mice with R-2×Aβ1–15 or 2×Aβ1–15 in combination with LT(R192G) adjuvant (Dickinson and Clements, 1995) induced anti-Aβ antibody titers 2–3 times higher than those achieved with aggregated, full-length Aβ40/42. Immunization with T1-R-Aβ1–15 or T1-Aβ1–15 plus LT(R192G) resulted in lower antibody levels. With all intranasal immunogens, a moderate-to-strong cellular immune response was detected against the immunogen in the absence of a cellular immune response against full-length Aβ. Antibody epitopes (Aβ1–7 or Aβ1–15), predominant immunoglobulin isotype (IgG2b), and recognition of plaques by antibodies from immunized mouse plasma on human AD brain sections were similar to antibodies induced by immunization with Aβ40/42. $hAPP_{FAD}$ mice (J20 line) immunized with R-2×Aβ1–15 or 2×Aβ1–15 also developed high antibody levels and antibody epitopes similar to wild-type mice, and showed a significant reduction of Aβ plaque load, significantly increased Aβ plasma levels, and a trend for lower insoluble cerebral Aβ by

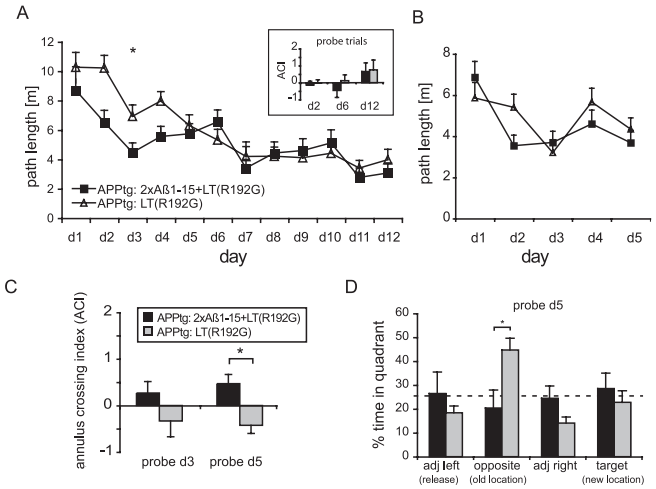

Figure 7. The effect of immunization with 2×Aβ1–15 plus LT(R192G) was assessed in a reference-memory version of the MWM. ***A***, 2×Aβ1–15 plus LT(R192G)-immunized $hAPP_{FAD}$ mice ($n = 6$) showed significantly faster learning acquisition during the first four training session of a 12 d test as compared with adjuvant-only-treated control $hAPP_{FAD}$ animals ($n = 7$; $p < 0.05$; days 1 to 5). Both cohorts of mice showed comparable spatial memory as evaluated by the ACI (defined as average frequency of swims over the platform site in the target quadrant minus average of swims over sites in other quadrants of the pool) at the end of training (***C***, inset). ***B***, During the learning reversal task, 2×Aβ1–15 plus LT(R192G)-immunized $hAPP_{FAD}$ mice showed a trend of faster initial acquisition of the new platform location as compared with control $hAPP_{FAD}$ mice during the first three training sessions ($p = 0.09$; days 1 to 3). During the reversal stage (days 4 and 5), both cohorts of mice showed a comparable response to platform displacement. ***C***, ACI during probe trials administered 1 h after training on days 3 and 5 in the platform reversal task. 2×Aβ1–15 plus LT(R192G)-immunized mice (black bars) show a positive ACI for the platform location on day 3 or day 5, whereas control $hAPP_{FAD}$ mice (gray bars) show a significantly lower and negative ACI. ***D***, Quadrant dwell times of probe-trial day 5 indicate that control $hAPP_{FAD}$ mice (gray bars) persevered with their search in the original, previous location of the pool. Asterisks indicate significant results ($p < 0.05$). Data are represented as mean ± SEM.

ELISA. Whereas in wild-type mice the Ig isotypes for the new immunogens included IgG2b, IgG2a, and IgG1, immunized $hAPP_{FAD}$ mice had a more Th2-biased humoral response resulting in higher titers of IgG2b and IgG1. Importantly, splenocytes from $hAPP_{FAD}$ mice immunized with R-2×Aβ1–15 or 2×Aβ1–15 did not react to full-length Aβ or Aβ1–15, indicating the potential for avoiding an Aβ-specific T-cell response. In addition, our results suggest that immunization of mice with 2×Aβ1–15 improved plasticity of acquisition of spatial information and spatial reference memory, as evaluated in the Morris water-maze test, as compared with age-matched control mice. Cognitive improvement tended to correlate with anti-Aβ titers in the immunized $hAPP_{FAD}$ mice.

Previously, we demonstrated that Aβ1–15 was not an effective primary immunogen, but was able to boost the immune response in WT mice after immunization with full-length Aβ (Leverone et al., 2003). In the present study, we show that a tandem repeat of Aβ1–15 was sufficient to effectively overcome this lack of immunogenicity. According to the high SI after restimulation of splenocytes with their immunogen and absence of proliferation after addition of Aβ1–15, one may speculate that this is attributable to the formation of a new, unknown T-cell epitope that is not present in a single sequence of Aβ1–15. Furthermore, it may also be attributable to its larger size, leading to less degradation, and presentation of a nonself sequence using the tandem repeat.

Addition of the RGD motif to the immunogens did not substantially increase antibody titers in long-term immunizations and was not able to replace the use of adjuvants as described for other immunogens (Yano et al., 2003). A consistent effect of RGD-containing immunogens is slightly higher SIs, indicative of a stronger cellular immune response (Figs. 4, 5). The fact that we did not detect a proliferative response against the RGD-peptide or the RGD-motif containing protein fibronectin in splenocyte cultures (data not shown) demonstrates that RGD did not act as a T-cell epitope. RGD is an integrin-binding and cell-attachment motif derived from cellular adhesion proteins such as fibronectin, collagen, fibrinogen, laminin, and many microbial proteins (Ruoslahti, 1988; Mecham, 1991; Ruoslahti, 1996). Therefore, the addition of RGD may increase uptake and transport through the mucous membrane by utilization of specific receptors (Ruoslahti, 1996), enhancing presentation of the antigen *in vivo*. However, splenocytes from R-2×Aβ1–15 immunized mice showed higher SI after restimulation with R-2×Aβ1–15 compared with 2×Aβ1–15, suggesting that RGD contributes to the secondary structure of the 2×Aβ1–15-containing immunogens by creating a new, slightly different T-cell epitope. Regardless of the mechanisms, RGD-containing peptides did not increase Aβ antibody levels but did accelerate antibody production.

Both Aβ1–15 tandem repeat immunogens significantly reduced total Aβ plaque load and increased Aβ plasma levels in $hAPP_{FAD}$ mice. In general, a more robust reduction was observed by immunohistochemical and Thioflavine S plaque labeling compared with the biochemical levels obtained by ELISA. This is likely because of the variability of Aβ levels between mice within each treatment group, resulting in a nonsignificant trend for reduced insoluble Aβ. However, reduced plaque burden corresponded with reduced TBS-insoluble Aβ fractions in brain homogenates. In contrast to R-2×Aβ1–15, 2×Aβ1–15 seemed to clear mainly Aβ1–42 and did not alter Aβ40 immunoreactivity, cerebral guanidinium-soluble Aβ40 levels, or Thioflavine S-positive plaque load. These differences between the immunogens may be because of high interanimal variability of Aβ plaque load or differences in the age when immunization was started. Alternatively, one may speculate that different Aβ clearance mechanisms may be involved. Different mechanisms of Aβ removal by antibodies have been proposed in the past (reviewed by Citron, 2004). They may include (1) Fc receptor (FcR)-mediated activation of microglia and subsequent phagocytosis of Aβ (Schenk et al., 1999; Bard et al., 2000; Bard et al., 2003), (2) the direct interaction of the antibody with Aβ deposits or aggregates leading to their disaggregation (Frenkel et al., 2000), and (3) transport of soluble Aβ into the plasma with a subsequent antibody-mediated degradation ("peripheral sink hypothesis") (DeMattos et al., 2001; Lemere et al., 2003). Recently, Deane et al. (2005) showed that anti-Aβ IgG increases Aβ clearance from the brain through effects on Aβ transport across the blood–brain barrier mediated by neonatal FcR (FcRn) or low-density lipoprotein receptor-related protein-dependent mechanisms (Deane et al., 2005). These mechanisms may be combined with other effects such as masking the proinflammatory and vasoactive effect of Aβ in the cerebrovasculature (Townsend et al., 2002) by antibodies, particularly in light of recent reports regarding brain-volume changes after Aβ immunotherapy (Fox et al., 2005). We observed increased levels of TBS-soluble Aβ after immunization with R-2×Aβ1–15, suggesting that perhaps the antibodies caused disaggregation of Aβ, presumably in the CNS, or alternatively, prevented the aggregation of Aβ over the immunization period. In addition, it is possible that the IgM titers in R-2×Aβ1–15-immunized animals may have contributed to the differences seen between the experiments, because IgM antibodies have been pro-

posed to contribute to clearance of plaques by a peripheral mechanism (Sigurdsson et al., 2004).

In the present study, we observed increased plasma Aβ levels in immunized animals, suggesting a shift of Aβ from the brain into the periphery leading to enhanced catabolism of Aβ as has been described previously (DeMattos et al., 2001). CD45 immunoreactivity, a marker for activated microglia, was reduced in R-2×Aβ1–15 immunized mice, whereas a slight increase was detected in 2×Aβ1–15 immunized animals. High levels of anti-Aβ antibodies may lead (temporarily) to activation of microglia as has been described for passive immunization (Wilcock et al., 2004a) leading to enhanced phagocytosis and degradation of cerebral Aβ via Fc receptor-mediated phagocytosis (Rogers et al., 2002). Although it has been reported that 0.1% of immunoglobulins cross the blood–brain barrier into the brain (Banks et al., 2002), colocalization of mouse IgG with cerebral plaques was not detected in our study, but this does not rule out the possibility that small numbers of antibodies crossed transiently into the CNS or were undetectable by our methods. It has been shown in many APP transgenic mouse models that fibrillar Aβ load correlates with activation of microglia (Frautschy et al., 1998; Gordon et al., 2002; Kitazawa et al., 2005). Consequently, we would expect to see relatively high levels of activated microglia in the mice immunized with 2×Aβ1–15, because their fibrillar plaque load was unchanged by immunization. In support of this effect, most activated microglia were found adjacent to or surrounding Aβ plaques.

Similar to our results with the tandem repeat immunogens, Bard and colleagues reported a reduction of amyloid and neuritic burden after immunization of PDAPP mice (transgenic mice carrying mutant human V717F APP under the PDGF promoter) with different N-terminal Aβ peptide fragments coupled to an ovalbumin T-cell epitope on a branched peptide framework (Bard et al., 2003). However, the specificity of the cellular immune response and amelioration of cognitive abilities were not addressed. Agadjanyan et al. (2005) reported that wild-type mice immunized with Aβ1–15 synthesized to a universal synthetic T-cell epitope PADRE (pan human leukocyte antigen DR-binding peptide), generated high anti-Aβ antibody levels in the absence of a T-cell response against full-length Aβ. Our data regarding immunization with R-2×Aβ1–15 and 2×Aβ1–15 confirm their findings and extend them to APP-tg mice. However, in our study, B6D2F1 wild-type mice immunized with immunogens containing the T1 Th-cell epitope did not induce anti-Aβ antibody levels above those observed with aggregated Aβ40/42. A strong cellular immune response against the immunogen was detected in the absence of splenocyte proliferation against full-length Aβ. Insertion of the T1 sequence at a different location (e.g., the C terminus of the immunogen) may improve antibody generation. The versatility of the T1 Th-cell epitope with different mouse MHC class II loci and different species make these immunogens an attractive candidate for additional studies in particular with other mouse strains or species. A recent publication analyzing gene expression profiles of patients from an AN-1792 immunization trial suggest reduced abilities to mount an effective immune response against Aβ, mainly because of the advanced age of the patients (O'Toole et al., 2005). Therefore, activation of the immune system in AD patients to mount an effective antibody response against Aβ and, in particular, to induce immunological memory, may require a strong universal T-cell epitope such as T1 that does not cross-react with Aβ T-cell epitope(s).

Cognitive evaluation of the immunization effects in our study showed a consistent and significant but rather subtle improvement of spatial reference memory acquisition, likely attributable to the small number of animals available for the study. Cognitive improvement was accompanied by a trend for reduced insoluble Aβ42, a significant reduction in Aβ42 hippocampal plaque burden, and a lack of change in fibrillar plaques, indicating that removal of primarily diffuse Aβ led to improved cognition. Our results also suggest improved plasticity of relearning of new information after immunization of $hAPP_{FAD}$ mice with 2×Aβ1–15, which is consistent with other studies evaluating learning and memory after Aβ immunization in the Morris water-maze task (Janus et al., 2000; Hartman et al., 2005), although a more pronounced effect of cognitive improvement was observed after Aβ immunization of younger mice (Jensen et al., 2005). The spatial memory measured in our probe trials showed a consistent trend to positively correlate with anti-Aβ antibody titers, additionally substantiating the notion that anti-Aβ antibodies have a beneficial effect on learning and memory.

Our data, together with reports from other researchers, demonstrate that immunogens containing N-terminal fragments of Aβ are sufficient for the production of high levels of specific antibodies. To our knowledge, our study is the first to characterize alternative immunogens that are able to induce high titers of anti-Aβ specific antibodies in the absence of a cellular immune response to full-length Aβ leading to a reduction of cerebral plaque burden and cognitive deficits in an AD animal model. We believe that these novel immunogens are promising candidates for a second-generation vaccine leading to an effective immunotherapy for AD while avoiding a potentially deleterious cellular immune response.

References

Agadjanyan MG, Ghochikyan A, Petrushina I, Vasilevko V, Movsesyan N, Mkrtichyan M, Saing T, Cribbs DH (2005) Prototype Alzheimer's disease vaccine using the immunodominant B cell epitope from β-amyloid and promiscuous T cell epitope pan HLA DR-binding peptide. J Immunol 174:1580–1586.

Ahlers JD, Takeshita T, Pendleton CD, Berzofsky JA (1997) Enhanced immunogenicity of HIV-1 vaccine construct by modification of the native peptide sequence. Proc Natl Acad Sci USA 94:10856–10861.

Banks WA, Terrell B, Farr SA, Robinson SM, Nonaka N, Morley JE (2002) Passage of amyloid beta protein antibody across the blood-brain barrier in a mouse model of Alzheimer's disease. Peptides 23:2223–2226.

Bard F, Cannon C, Barbour R, Burke RL, Games D, Grajeda H, Guido T, Hu K, Huang J, Johnson-Wood K, Khan K, Kholodenko D, Lee M, Lieberburg I, Motter R, Nguyen M, Soriano F, Vasquez N, Weiss K, Welch B, et al. (2000) Peripherally administered antibodies against amyloid beta-peptide enter the central nervous system and reduce pathology in a mouse model of Alzheimer disease. Nat Med 6:916–919.

Bard F, Barbour R, Cannon C, Carretto R, Fox M, Games D, Guido T, Hoenow K, Hu K, Johnson-Wood K, Khan K, Kholodenko D, Lee C, Lee M, Motter R, Nguyen M, Reed A, Schenk D, Tang P, Vasquez N, et al. (2003) Epitope and isotype specificities of antibodies to beta-amyloid peptide for protection against Alzheimer's disease-like neuropathology. Proc Natl Acad Sci USA 100:2023–2028.

Cain D, Beiko J, Boon F (1997) Navigation in the water maze: the role of proximal and distal visual cues, path integration, and magnetic field information. Psychobiology 25:286–293.

Cease KB, Margalit H, Cornette JL, Putney SD, Robey WG, Ouyang C, Streicher HZ, Fischinger PJ, Gallo RC, DeLisi C, Berzofsky JA (1987) Helper T-cell antigenic site identification in the acquired immunodeficiency syndrome virus gp120 envelope protein and induction of immunity in mice to the native protein using a 16-residue synthetic peptide. Proc Natl Acad Sci USA 84:4249–4253.

Citron M (2004) Strategies for disease modification in Alzheimer's disease. Nat Rev Neurosci 5:677–685.

Cribbs D, Ghochikyan A, Vasilevko V, Tran M, Petrushina I, Sadzikava N, Babikyan D, Kesslak P, Kieber-Emmons T, Cotman C, Agadjanyan M

(2003) Adjuvant-dependent modulation of Th1 and Th2 responses to immunization with beta-amyloid. Int Immunol 15:505–514.

Deane R, Sagare A, Hamm K, Parisi M, LaRue B, Guo H, Wu Z, Holtzman DM, Zlokovic BV (2005) IgG-assisted age-dependent clearance of Alzheimer's amyloid β peptide by the blood–brain barrier neonatal Fc receptor. J Neurosci 25:11495–11503.

DeMattos RB, Bales KR, Cummins DJ, Dodart JC, Paul SM, Holtzman DM (2001) Peripheral anti-A beta antibody alters CNS and plasma A beta clearance and decreases brain A beta burden in a mouse model of Alzheimer's disease. Proc Natl Acad Sci USA 98:8850–8855.

Dickinson BL, Clements JD (1995) Dissociation of *Escherichia coli* heat-labile enterotoxin adjuvanticity from ADP-ribosyltransferase activity. Infect Immun 63:1617–1623.

Dodart J-C, Bales K, Gannon K, Greene S, DeMattos R, Mathis C, DeLong C, Wu S, Wu X, Holtzman D, Paul S (2002) Immunization reverses memory deficits without reducing brain Aβ burden in Alzheimer's disease model. Nat Neurosci 5:452–457.

Ferrer I, Boada Rovira M, Sanchez Guerra ML, Rey MJ, Costa-Jussa F (2004) Neuropathology and pathogenesis of encephalitis following amyloid-beta immunization in Alzheimer's disease. Brain Pathol 14:11–20.

Fox NC, Black RS, Gilman S, Rossor MN, Griffith SG, Jenkins L, Koller M (2005) Effects of Aβ immunization (AN1792) on MRI measures of cerebral volume in Alzheimer disease. Neurology 64:1563–1572.

Frautschy SA, Yang F, Irrizarry M, Hyman B, Saido TC, Hsiao K, Cole GM (1998) Microglial response to amyloid plaques in APPsw transgenic mice. Am J Pathol 152:307–317.

Frenkel D, Katz O, Solomon B (2000) Immunization against Alzheimer's beta-amyloid plaques via EFRH phage administration. Proc Natl Acad Sci USA 97:11455–11459.

Gilman S, Koller M, Black RS, Jenkins L, Griffith SG, Fox NC, Eisner L, Kirby L, Boada Rovira M, Forette F, Orgogozo JM (2005) Clinical effects of Aβ immunization (AN1792) in patients with AD in an interrupted trial. Neurology 64:1553–1562.

Gordon MN, Holcomb LA, Jantzen PT, DiCarlo G, Wilcock D, Boyett KW, Connor K, Melachrino J, O'Callaghan JP, Morgan D (2002) Time course of the development of Alzheimer-like pathology in the doubly transgenic PS1+APP mouse. Exp Neurol 173:183–195.

Hardy J, Selkoe DJ (2002) The amyloid hypothesis of Alzheimer's disease: progress and problems on the road to therapeutics. Science 297:353–356.

Hart MK, Palker TJ, Matthews TJ, Langlois AJ, Lerche NW, Martin ME, Scearce RM, McDanal C, Bolognesi DP, Haynes BF (1990) Synthetic peptides containing T and B cell epitopes from human immunodeficiency virus envelope gp120 induce anti-HIV proliferative responses and high titers of neutralizing antibodies in rhesus monkeys. J Immunol 145:2677–2685.

Hartman RE, Izumi Y, Bales KR, Paul SM, Wozniak DF, Holtzman DM (2005) Treatment with an amyloid-β antibody ameliorates plaque load, learning deficits, and hippocampal long-term potentiation in a mouse model of Alzheimer's disease. J Neurosci 25:6213–6220.

Haynes BF, Arthur LO, Frost P, Matthews TJ, Langlois AJ, Palker TJ, Hart MK, Scearce RM, Jones DM, McDanal C (1993) Conversion of an immunogenic human immunodeficiency virus (HIV) envelope synthetic peptide to a tolerogen in chimpanzees by the fusogenic domain of HIV gp41 envelope protein. J Exp Med 177:717–727.

Janus C (2004) Search strategies used by APP transgenic mice during navigation in the Morris water maze. Learn Mem 11:337–346.

Janus C, Pearson J, McLaurin J, Mathews PM, Jiang Y, Schmidt SD, Chishti MA, Horne P, Heslin D, French J, Mount HT, Nixon RA, Mercken M, Bergeron C, Fraser PE, St George-Hyslop P, Westaway D (2000) A beta peptide immunization reduces behavioural impairment and plaques in a model of Alzheimer's disease. Nature 408:979–982.

Jensen MT, Mottin MD, Cracchiolo JR, Leighty RE, Arendash GW (2005) Lifelong immunization with human beta-amyloid (1–42) protects Alzheimer's transgenic mice against cognitive impairment throughout aging. Neuroscience 130:667–684.

Johnson Jr WC (1990) Protein secondary structure and circular dichroism: a practical guide. Proteins 7:205–214.

Kitazawa M, Oddo S, Yamasaki TR, Green KN, LaFerla FM (2005) Lipopolysaccharide-induced inflammation exacerbates tau pathology by a cyclin-dependent kinase 5-mediated pathway in a transgenic model of Alzheimer's disease. J Neurosci 25:8843–8853.

Lee M, Bard F, Johnson-Wood K, Lee C, Hu K, Griffith SG, Black RS, Schenk D, Seubert P (2005) Abeta42 immunization in Alzheimer's disease generates Abeta N-terminal antibodies. Ann Neurol 58:430–435.

Lemere C, Spooner E, LaFrancois J, Malester B, Mori C, Leverone J, Matsuoka Y, DeMattos R, Holtzman D, Clements J, Selkoe D, Duff K (2003) Evidence for peripheral clearance of Aβ following chronic, active Aβ immunization in PSAPP mice. Neurobiol Dis 14:10–18.

Lemere CA, Maron R, Spooner ET, Grenfell TJ, Mori C, Desai R, Hancock WW, Weiner HL, Selkoe DJ (2000) Nasal A beta treatment induces anti-A beta antibody production and decreases cerebral amyloid burden in PD-APP mice. Ann NY Acad Sci 920:328–331.

Lemere CA, Spooner ET, Leverone JF, Mori C, Clements JD (2002) Intranasal immunotherapy for the treatment of Alzheimer's disease: *Escherichia coli* LT and LT(R192G) as mucosal adjuvants. Neurobiol Aging 23:991–1000.

Lemere CA, Beierschmitt A, Iglesias M, Spooner ET, Bloom JK, Leverone JF, Zheng JB, Seabrook TJ, Louard D, Li D, Selkoe DJ, Palmour RM, Ervin FR (2004) Alzheimer's disease abeta vaccine reduces central nervous system abeta levels in a non-human primate, the Caribbean vervet. Am J Pathol 165:283–297.

Leverone JF, Spooner ET, Lehman HK, Clements JD, Lemere CA (2003) Abeta1–15 is less immunogenic than Abeta1–40/42 for intranasal immunization of wild-type mice but may be effective for "boosting." Vaccine 21:2197–2206.

Levites Y, Das P, Price RW, Rochette MJ, Kostura LA, McGowan EM, Murphy MP, Golde TE (2006) Anti-Abeta(42)- and anti-Abeta(40)-specific mAbs attenuate amyloid deposition in an Alzheimer disease mouse model. J Clin Invest 116:193–201.

Maier M, Seabrook TJ, Lemere CA (2005a) Developing novel immunogens for an effective, safe Alzheimer's disease vaccine. Neurodegenerative Dis 2:267–272.

Maier M, Seabrook TJ, Lemere CA (2005b) Modulation of the humoral and cellular immune response in Abeta immunotherapy by the adjuvants monophosphoryl lipid A (MPL), cholera toxin B subunit (CTB) and *E. coli* enterotoxin LT(R192G). Vaccine 23:5149–5159.

Masliah E, Hansen L, Adame A, Crews L, Bard F, Lee C, Seubert P, Games D, Kirby L, Schenk D (2005) Abeta vaccination effects on plaque pathology in the absence of encephalitis in Alzheimer disease. Neurology 64:129–131.

McLaurin J, Cecal R, Kierstead M, Tian X, Phinney A, Manea M, French J, Lambermon M, Darabie A, Brown M, Janus C, Chishti M, Horne P, Westaway D, Fraser P, Mount H, Przybylski M, St George-Hyslop P (2002) Therapeutically effective antibodies against amyloid-beta peptide target amyloid-beta residues 4–10 and inhibit cytotoxicity and fibrillogenesis. Nat Med 8:1263–1269.

Mecham RP (1991) Laminin receptors. Annu Rev Cell Biol 7:71–91.

Monsonego A, Maron R, Zota V, Selkoe DJ, Weiner HL (2001) Immune hyporesponsiveness to amyloid beta-peptide in amyloid precursor protein transgenic mice: implications for the pathogenesis and treatment of Alzheimer's disease. Proc Natl Acad Sci USA 98:10273–10278.

Monsonego A, Zota V, Karni A, Krieger JI, Bar-Or A, Bitan G, Budson AE, Sperling R, Selkoe DJ, Weiner HL (2003) Increased T cell reactivity to amyloid beta protein in older humans and patients with Alzheimer disease. J Clin Invest 112:415–422.

Morgan D, Diamond DM, Gottschall PE, Ugen KE, Dickey C, Hardy J, Duff K, Jantzen P, DiCarlo G, Wilcock D, Connor K, Hatcher J, Hope C, Gordon M, Arendash GW (2000) A beta peptide vaccination prevents memory loss in an animal model of Alzheimer's disease. Nature 408:982–985.

Morris RG, Garrud P, Rawlins JN, O'Keefe J (1982) Place navigation impaired in rats with hippocampal lesions. Nature 297:681–683.

Mucke L, Masliah E, Yu G-Q, Mallory M, Rockenstein EM, Tatsuno G, Hu K, Kholodenko D, Johnson-Wood K, McConlogue L (2000) High-level neuronal expression of Aβ1–42 in wild-type human amyloid protein precursor transgenic mice: synaptotoxicity without plaque formation. J Neurosci 20:4050–4058.

Nicoll JA, Wilkinson D, Holmes C, Steart P, Markham H, Weller RO (2003) Neuropathology of human Alzheimer disease after immunization with amyloid-beta peptide: a case report. Nat Med 9:448–452.

Oishi Y, Onozuka A, Kato H, Shimura N, Imai S, Nisizawa T (2001) The effect of amino acid spacers on the antigenicity of dimeric peptide-inducing cross-reacting antibodies to a cell surface protein antigen of Streptococcus mutans. Oral Microbiol Immunol 16:40–44.

Orgogozo JM, Gilman S, Dartigues JF, Laurent B, Puel M, Kirby LC, Jouanny P, Dubois B, Eisner L, Flitman S, Michel BF, Boada M, Frank A, Hock C (2003) Subacute meningoencephalitis in a subset of patients with AD after Abeta42 immunization. Neurology 61:46–54.

O'Toole M, Janszen DB, Slonim DK, Reddy PS, Ellis DK, Legault HM, Hill AA, Whitley MZ, Mounts WM, Zuberek K, Immermann FW, Black RS, Dorner AJ (2005) Risk factors associated with beta-amyloid(1–42) immunotherapy in preimmunization gene expression patterns of blood cells. Arch Neurol 62:1531–1536.

Pfeifer M, Boncristiano S, Bondolfi L, Stalder A, Deller T, Staufenbiel M, Mathews PM, Jucker M (2002) Cerebral hemorrhage after passive anti-Abeta immunotherapy. Science 298:1379.

Racke MM, Boone LI, Hepburn DL, Parsadainian M, Bryan MT, Ness DK, Piroozi KS, Jordan WH, Brown DD, Hoffman WP, Holtzman DM, Bales KR, Gitter BD, May PC, Paul SM, DeMattos RB (2005) Exacerbation of cerebral amyloid angiopathy-associated microhemorrhage in amyloid precursor protein transgenic mice by immunotherapy is dependent on antibody recognition of deposited forms of amyloid β. J Neurosci 25:629–636.

Rogers J, Strohmeyer R, Kovelowski C, Li R (2002) Microglia and inflammatory mechanisms in the clearance of amyloid beta peptide. Glia 40:260–269.

Ruoslahti E (1988) Fibronectin and its receptors. Annu Rev Biochem 57:375–413.

Ruoslahti E (1996) RGD and other recognition sequences for integrins. Annu Rev Cell Dev Biol 12:697–715.

Schenk D, Barbour R, Dunn W, Gordon G, Grajeda H, Guido T, Hu K, Huang J, Johnson-Wood K, Khan K, Kholodenko D, Lee M, Liao Z, Lieberburg I, Motter R, Mutter L, Soriano F, Shopp G, Vasquez N, Vendevert C, et al. (1999) Immunization with amyloid-beta attenuates Alzheimer-disease-like pathology in the PDAPP mouse. Nature 400:173–177.

Seabrook TJ, Bloom JK, Iglesias M, Spooner ET, Walsh DM, Lemere CA (2004) Species-specific immune response to immunization with human versus rodent A beta peptide. Neurobiol Aging 25:1141–1151.

Sigurdsson EM, Knudsen E, Asuni A, Fitzer-Attas C, Sage D, Quartermain D, Goni F, Frangione B, Wisniewski T (2004) An attenuated immune response is sufficient to enhance cognition in an Alzheimer's disease mouse model immunized with amyloid-β derivatives. J Neurosci 24:6277–6282.

Town T, Tan J, Sansone N, Obregon D, Klein T, Mullan M (2001) Characterization of murine immunoglobulin G antibodies against human amyloid-β1–42. Neurosci Lett 307:101–104.

Townsend KP, Obregon D, Quadros A, Patel N, Volmar C, Paris D, Mullan M (2002) Proinflammatory and vasoactive effects of Abeta in the cerebrovasculature. Ann NY Acad Sci 977:65–76.

Walsh DM, Selkoe DJ (2004) Deciphering the molecular basis of memory failure in Alzheimer's disease. Neuron 44:181–193.

Weiner HL, Lemere CA, Maron R, Spooner ET, Grenfell TJ, Mori C, Issazadeh S, Hancock WW, Selkoe DJ (2000) Nasal administration of amyloid-beta peptide decreases cerebral amyloid burden in a mouse model of Alzheimer's disease. Ann Neurol 48:567–579.

Wilcock DM, Rojiani A, Rosenthal A, Levkowitz G, Subbarao S, Alamed J, Wilson D, Wilson N, Freeman MJ, Gordon MN, Morgan D (2004a) Passive amyloid immunotherapy clears amyloid and transiently activates microglia in a transgenic mouse model of amyloid deposition. J Neurosci 24:6144–6151.

Wilcock DM, Rojiani A, Rosenthal A, Subbarao S, Freeman MJ, Gordon MN, Morgan D (2004b) Passive immunotherapy against Abeta in aged APP-transgenic mice reverses cognitive deficits and depletes parenchymal amyloid deposits in spite of increased vascular amyloid and microhemorrhage. J Neuroinflammation 1:24.

Yano A, Onozuka A, Matin K, Imai S, Hanada N, Nisizawa T (2003) RGD motif enhances immunogenicity and adjuvanticity of peptide antigens following intranasal immunization. Vaccine 22:237–243.